In the Balance: Natural vs. Embanked Landscapes on the Ganges Brahmaputra Tidal Delta Plain

By

Leslie Elaine Wallace Auerbach

Thesis

Submitted to the Faculty of the

Graduate School of Vanderbilt University

in partial fulfillment of the requirements

for the degree of

MASTER OF SCIENCE

in

Earth and Environmental Sciences

December, 2013

Nashville, Tennessee

Approved:

Steven Goodbred, Ph.D.

Ralf Bennartz, Ph.D.

To my son Reid, the light of my life

and

To my late Godfather, John Waldman

ACKNOWLEDGEMENTS

This work was made possible by the financial support of the Office of Naval Research. I am especially grateful to my advisor, Dr. Steven Goodbred, for his infectious enthusiasm for Bangladesh and the Ganges-Brahmaputra Delta. His guidance and advice regarding this research has been invaluable and his encouragement of my academic and career goals is truly appreciated. I am also indebted to my other committee members, Dr. David Furbish and Dr. Molly Miller, for their advice throughout this research. Finally, I am grateful to Dr. Ralf Bennartz for his constructive feedback as a second reader of this work.

I am also grateful to the staff and students in the Department of Earth and Environmental Sciences. In particular, Dr. Carol Wilson has been an unending source of advice, moral support and friendship. Much of this work would not have been completed without the field support of Carol and Jennifer Pickering. I am also grateful to Greg George and Laura Benneyworth for their advice and friendship. I am forever indebted to our Dhaka University and Khulna University colleagues, including Dhiman Mondal, Saddam Hossain, Basudeb Kumar, Kazi Rifat Ahmed, Farjana Akter and Zitu Karim. Their field support, local perspectives, and friendship are one of a kind.

No one has provided more encouragement and support throughout this experience than my family. My loving husband, Scott, has never waivered in his support of my dreams, academic or otherwise. I am eternally grateful to my mom and dad for the countless sacrifices they have made to ensure that I could spend the rest of my life getting paid to play in the mud. I am also thankful for my son, Reid, who is living proof that you really can have it all.

Finally, I am forever grateful to the people of Polder 32. In the midst of enormous hardship, they always welcomed me with warm, friendly smiles. They gave this research special purpose and I am so humbled by my experiences and interactions with the hard-working people of the tidal delta plain.

TABLE OF CONTENTS

LIST OF TABLES

LIST OF FIGURES

LIST OF ABBREVIATIONS

1. GPS - Global Positioning System
2. UNESCO - United Nations Education, Scientific and Cultural Organization
3. EGM96 - Earth Gravitation Model 1996
4. GAMIT - GPS At Massachusetts Institute of Technology
5. ITRF - International Terrestrial Reference Frame
6. GLOBK - Global Kalman
7. VLBI - Very Long Baseline Interferometry
8. IGS - International GPS Service
9. RSL - Relative Sea Level
10. IPCC - Intergovernmental Panel on Climate Change

Introduction

The Ganges-Brahmaputra (G-B) river delta, with 150 million people and a vast, low-lying coastal plain, is among the world's delta systems perceived to be at great risk to degradation and submergence under multiple climate and sea-level rise scenarios (Bhuiyan and Dutta, 2012; Dasgupta et al., 2011; IPCC, 2007; Syvitski et al., 2009). Pristine areas of the G-B delta such as the Sundarbans mangrove forest, however, have remained stable through recent and late Holocene times, sustained by a network of fluvial and tidal channels that effectively disperse the immense riverine sediment load (Allison, 1998; Goodbred and Kuehl, 1999). Areas of the human-altered landscape have not faired as well, experiencing a net elevation loss of at least 1 m since being embanked in the 1960s. The acute effects of this elevation offset were felt in 2009 when the embankments of several large islands failed during Cyclone Aila, leaving >100 km^2 of land tidally inundated for nearly two years until embankments were repaired. Despite sustained human suffering during this time, the newly reconnected landscape rebounded with tens of centimeters of tidally deposited sediment, accounting for decades-worth of normal sedimentation, but only partly restoring the elevation lost over the previous five decades. Nevertheless, most embanked landscapes in southwest Bangladesh now lie well below mean high water and are already at considerable risk of severe flooding, regardless of future global change scenarios. Based on these observations, I hypothesize that agents of environmental change, specifically human modifications of the landscape, are capable of altering the natural sediment budget of the G-B tidal delta plain. In doing so, regions of the human-modified tidal delta plain are susceptible to impeded sediment delivery and rapid elevation loss, while pristine regions of the tidal delta plain are able to keep pace with regional rates of sea level rise. If confirmed, these findings would demonstrate that local sediment-dispersal processes and land use practices, in addition to regional-scale variables, will strongly influence the future of the G-B tidal delta plain.

Research Objectives and General Approach

The overarching goal of the research is to understand the role that human-modifications of the environment play in determining physical landscape processes and evolution. This study aims to address the following:

1. Document the elevation offset across Polder 32 by conducting a GPS elevation survey across the polder and the Sundarbans.
2. Address the roles of sediment accretion, eustatic sea level rise, compaction and subsidence in producing the elevation offset.
3. Identify causes of Polder 32 embankment failure, which led to a partial recovery of the lost elevation, by digitizing historical shoreline imagery.
4. Compare landscape evolution in the human-modified and pristine environments, which should reveal the important differences in sediment delivery and subsequent landscape elevations and relative sea levels.

This report is organized such that the approach, methods, results and discussion of each of the four main objectives are addressed individually, followed by a discussion of the broad conclusions drawn from results of the four-part study.

Background

The land-sea interface is constantly evolving as sediment input, tidal transport processes, and sea level fluctuate. River deltas lie in a particularly delicate balance between the marine and terrestrial environments, and the future of these systems is dictated by the flux and dispersal of sediment that ultimately determines delta-system response to environmental change. Although the risks of environmental change and sea-level rise to fluvial delta systems are widely recognized (Day et al., 1995; Ericson et al., 2006; IPCC, 2007; Syvitski et al., 2009), a collective understanding of local conditions, processes, and responses within these complex landscapes are often poorly known (Ericson et al., 2006; Overeem and Syvitski, 2009; Syvitski et al., 2009). This is particularly true of the Ganges-Brahmaputra (G-B) delta (Fig. 1), which is constructed by the 1 billion tons of sediment transported annually from the Himalayan highlands to the Bay of Bengal, primarily during the May-October Indian monsoon (Milliman and Syvitski, 1992) (Fig. 2).

River Channel History

During the late Holocene, the Ganges distributaries migrated eastward to the present location of the G-B delta front and the western delta lobe was isolated from fluvial interaction (Allison, 1998; Allison et al., 2003).

Though abandoned by the fluvial system, this western lobe is comprised of numerous islands dissected by a network of large shore-normal tidal distributaries, many smaller connecting channels, and a dendritic system of shallow creeks draining the islands (Fig. 3). In the present delta configuration, approximately one half of the annual G-B sediment load is deposited onto the lower delta plain and inner shelf, leading to net land construction through at least the past two centuries (Allison, 1998). The semi-diurnal tides transport about 15% of the suspended sediment derived from silt-laden plumes on the inner shelf and redeposit the sediment back onto the abandoned western lobe, which is the primary source of sediment aggradation for the tidal platform (Allison and Kepple, 2001; Goodbred and Kuehl, 1999; Rogers et al., 2013). This documented pattern of regional sediment distribution suggests that sediment accretion on the lower G-B tidal delta plain is likely in a stable but dynamic equilibrium with sea level rise during the late Holocene.

Natural and Human-modified Tidal Landscapes

The Sundarbans mangrove forest, a 10,000 km^2 UNESCO World Heritage site, comprises the pristine area of the delta and provides a laboratory and record of the natural delta evolution (Fig. 3). The Sundarbans extends from the coast to 80 km inland and periodic tidal inundation moves sediment from the tidal distributaries onto the landscape. Allison (2001) and Rogers et al. (2013) report an average sediment accretion rate of 1 cm/yr in the Sundarbans. This accretion has maintained the elevation of this part of the tidal delta plain for millennia, with an average of only 4 km^2/yr land loss during the last two centuries (balanced by a net gain of 12 km^2/yr in the eastern delta (Allison, 1998). Overall the physical environment of the Sundarbans remains robust with no major land loss or conversion to open water, such as that occurring in other delta systems like the Mississippi and Nile (Bourne, 2000; Giri et al., 2007; Stanley and Warne, 1998).

Bordering the pristine Sundarbans to the north is a starkly contrasting, human-modified environment that comprises a total of 56 islands, formerly forested and intertidal. The islands were cleared and ultimately embanked in the 1960s and 1970s as part of a largely successful effort to relieve famine by increasing arable land for rice paddy cultivation (Rahman, 1994). Referred to by their Dutch name, *polder*, these islands are normally protected from tidal and storm-surge inundation by earthen embankments constructed around the island margins. However, in addition to stemming floodwater, the embankments also preclude the deposition of sediment and organic matter that normally sustains the elevation and fertility of the landscape.

Historical imagery of the tidal delta plain reveals that poldered regions are susceptible to widespread, multi-year flooding events, leaving the landscape tidally inundated and presumably incapable of maintaining human lives and livelihoods. Google Earth imagery reveals that Polder 32, a 60-km^2 island in the Dacope upazilla of Bangladesh's Khulna division adjacent to the Sundarbans, was tidally inundated for almost two years following Cyclone Aila, a category one cyclone which struck West Bengal, India, and southwest Bangladesh on May 25, 2009 (Fig. 4). Field observations in May 2012 indicate that Polder 32 was flooded as a result of a series of embankment breaches during Cyclone Aila. Observations also reveal a 1-1.5m elevation offset of the interior poldered landscape relative to mean high water levels (Fig. 5).

1. Land Surface Elevation

1.1 Approach and Methods

Observations indicate that the Sundarbans is flooded during spring high tides with a total inundation period of approximately 2 hours per day. Poldered landscapes, however, have been observed at elevations lower than mean high water levels outboard of the embankments. An elevation offset was observed in multiple locations on Polder 32 in May 2012. To document the magnitude and spatial extent of the offset, this study implemented a series of GPS elevation survey transects to record elevations of the poldered and adjacent pristine environments.

A combination Fast Static GPS – optical leveling survey was conducted in May 2012 to establish absolute land surface elevations on Polder 32 and the adjacent Sundarbans. Measured elevations were benchmarked relative to the EGM96 datum. The survey was conducted using two fixed base stations and one rover to triangulate elevation values with cm-scale error. The fixed base stations included Trimble NetR9 receivers with Zephyr II antennas installed on the polder. One antenna was cemented into the roof of a reinforced concrete school building (Fig. 6) and the second antenna was mounted on a heavy steel fixed-height tripod. Continuous GPS data for both base stations were processed using GAMIT version 10.4 (Herring et al., 2010a, 2010b) to produce position in the ITRF2008 reference frame, and the positions were stabilized using GLOBK filter VLBI and GPS analysis program Version 10.1 (Herring et al., 2010a, 2010b) with 21 IGS sites. The rover, also a Trimble NetR9 with a Zephyr II antenna, was mounted on a fixed height tripod (Fig. 6). Minimum observation times of the rover at each site were 10 minutes. Alongside the rover, a theodolite positioned on the embankment top measured the relative elevations of the land

inside and outside of the embankment relative to the embankment top and antenna. Theodolite measurements tied to the GPS survey were used to record interior polder elevations. The same method was used to collect elevation data along two transects in the Sundarbans. The elevation data were processed using Trimble Business Center and all elevations are relative to mean sea level using the EGM96 geoid model. Base station errors were less than 2 cm and median errors for GPS points was 4 cm with errors above 10 cm at three stations.

1.2 Results

Results of the GPS elevation survey transects (Fig. 7) show that the Sundarbans tidal platform is positioned at +2.65 m relative to the EGM96 datum. These elevations are consistent within hundreds of meters of the riverbank and thus do not indicate bias from natural levee formation or proximity to the tidal channel, which is only 50 m wide. Around the margin of Polder 32, river-bank terraces located outboard of the embankments are positioned at approximately the same elevation as the Sundarbans, with heights measured at X locations around the polder ranging in elevation from XX to XX m (Fig. 7.) Embankment top elevations, documented at X locations on Polder 32, ranged from +3.7 to +4.6 m (Fig. 7). The interior poldered landscape elevation was recorded at XX locations on the polder. The elevation of the embanked landscape is +1.5 m relative to EGM96, which is >1 m lower than elevations of river-bank terraces outside of the embankments or in the pristine Sundarbans (Fig.7). The range of elevations on the interior polder is XX to XX m, indicating that these low elevations are consistent throughout the 60 km^2 of the island (Fig. 7). Theodolite errors were less than 1cm. Post-storm sedimentation has not been subtracted from the measured elevations due to heterogeneities in both the deposit thickness and pre-existing topography, which would introduce an unknown degree of error. While topographic variability may contribute to slight variations in polder elevations, the elevation offset noted in field investigations was polder-wide.

1.3 Discussion

The similarity in elevation between the Sundarbans and the river-bank terraces around Polder 32 suggests that these regularly flooded settings are in a similar steady-state condition between sediment accretion and relative sea-level rise. The steady-state condition of these regularly flooded landscapes reflects the immense sediment supply and robust nature of unembanked regions of the tidal delta plain. The range in embankment top elevations recorded in the elevation survey reflects variations in construction style, with concrete structures generally positioned at higher elevations than earthen embankments. The mean elevation of the interior poldered landscape, +1.5 m, is more than 1 m lower than river-bank terraces and the Sundarbans platform. This elevation disparity represents an average loss of ~2 cm/yr of relative sea-level in the five decades since polder construction. This rate of effective sea-level rise is more than twice the upper end of the IPCC projections for future sea-level rise, making these poldered landscapes a very useful, albeit troubling, analog for studying the impact of increased sea-level rise in coming decades (IPCC, 2007).

2. Relative Sea Level

2.1 Approach and Methods

Relative changes between the local land-surface elevation and water levels (ΔRSL) are defined by the rates of sediment accretion (A), eustatic sea-level rise (ΔE), compaction (C), and tectonic subsidence (M), as:

$$\Delta RSL = A - (\Delta E + C + M)$$

Syvitski et al. (2009) estimated values for these variables within delta systems worldwide to compile an index of vulnerability (Syvitski et al., 2009). This approach has brought attention to the vulnerability of deltaic systems, particularly the role that humans and human-induced modifications may play. Based on the model of Syvitski et al. (2009), the G-B delta is among the 33 deltas worldwide at risk to a 50% increase in severe flooding over the next century as a result of relative sea-level rise. However, deltaic systems are complex and not uniform, exhibiting considerable spatial and temporal heterogeneity in their rates of sediment aggradation, compaction, and subsidence that define vulnerability. This study aims to constrain the variables which contribute to relative sea-level rise in the tidal delta plain of Bangladesh, and specifically to address the differences in human-modified and pristine landscapes in this region. In addition to making local estimations of these variables, this study accounts for land-surface compaction resulting from wood extraction (W), as roots and stumps were removed for fuel and improved tilling following deforestation.

Average sediment accretion rates of 1 cm/yr in the Sundarbans have been documented by Allison and Kepple (2001) and by Rogers et al. (2013). Using methods similar to those used in the Sundarbans by Rogers et al. (2013), this study attempts to record sedimentation rates on the outboard river-bank terraces of Polder 32 using sediment traps. These traps consisted of a ceramic tile and artificial turf used to collect sediments deposited by the

tides; however, disturbances and removal of trap materials by the local population resulted in no recovery of sediment traps deployed on Polder 32. On the interior poldered landscape, sediment accretion prior to embankment failure was assumed to be zero because of embankment protection from tidal inundation. The recent depositional history of the human-modified and pristine environments was confirmed with a 0.5 m-long gouge auger, which was used to collect sediment cores to 1.5 m depth at 114 locations on Polder 32, 11 sites on adjacent polders, and 2 sites in the Sundarbans. Cores were collected along the GPS elevation survey transects to facilitate comparison of lithologic and topographic features of the landscape.

Rates of eustatic sea level rise, compaction and tectonic subsidence in the Sundarbans were derived from previously published studies and from coastal tide gauge records obtained from the Bangladesh Water Development Board. Compaction rates on Polder 32, which are the most difficult variable to constrain due to human activities, were estimated in this study based on preliminary compaction data from the Sundarbans. The elevation loss associated with reduced root biomass during deforestation was calculated using documented allometric equations (Komiyama et al., 2005). Komiyama et al. (2005) calculate the root biomass based on the weight of mangrove trunk, leaf, and above-ground and below-ground root biomass. Mangrove root weight (W_R) (kg) is calculated as:

$$W_R = 0.199\rho^{0.899}D^{2.22}$$

where ρ (t/m^3) is wood density and D (m) is trunk diameter at ~1.3 m height (Komiyama et al., 2005). Measurements from approximately 40 mangrove trees, including *Heritiera fomes, Xylocarpus mekongensis, Avicennia* sp., *Bruguiera gymnorrhiza*, and *Sonneratia apetala,* were obtained in the Sundarbans (Table 1). Root volume (W_v) was calculated as:

$$(W_v) = W_R / 1000*\rho.$$

2.2 Results

The results of the relative sea level calculation for the pristine and human-modified environments, which include original data and values obtained from the literature, are shown in Table 2. Sediment accretion rates in the Sundarbans are reported by Allison and Kepple (2001) to range from 0.06-2.1 cm/yr, with an average of 1 cm/yr (Table 2). Rogers et al. (2013) also document average accretion rates of 1 cm/yr in the Sundarbans (Table 2). Coastal tide gauge records from 1975 to 2005 constrain the background relative sea level rise (Fig. 11) to 0.6 cm/yr (Table 2). Global mean sea level rise, reported by the IPCC (2007), contributes 0.2 – 0.4 cm/yr with a mean of 0.3 cm/yr (Table 2). Compaction is likely the least constrained variable in the relative sea level budget of G-B tidal delta plain, with estimated values in the pristine environment potentially ranging from 0.1 to 0.8 cm/yr (Table 2). Recent preliminary results from fiber-optic cables installed in the G-B delta indicate natural compaction rates of 0.4 cm/yr in the upper 10 m of sediment (Table 2). Allison and Kepple (2001) estimate compaction-induced subsidence rates of 0.1-0.4 cm/yr (Table 2). Estimated mean compaction and subsidence values of 0.4 cm/yr are used in this study (Table 2). The resulting mean *ΔRSL* for the Sundarbans tidal delta plain sums to ~0.0 cm/yr, reflecting the known condition that sediment accretion has maintained equilibrium with relative sea-level rise in this historically stable landscape (Allison, 1998) (Table 2).

On Polder 32, sediment accretion is estimated at 0 cm/yr due to embankment protection, which precludes sediment delivery to the landscape. The mean rate of eustatic sea level rise remains the same at 0.3 cm/yr. Mean anthropogenic compaction rates on Polder 32 are estimated in this study to be 0.8 cm/yr, approximately double that of the natural compaction rate of the Sundarbans (Table 2). First-order estimates of elevation lost via wood extraction (Table 2) suggest that the sum of root volume (302.2 m^3) divided by the area surveyed (~1500 m^2) yields depth taken up by roots (~20 cm) (Tables 1 and 2). In contrast to the Sundarbans, RSL values for the sediment-starved polder sum to –1.5 cm/yr, which includes anthropogenically-enhanced rates of compaction caused by the drying of shallow soils and the extraction of wood. In total these rates account for ~95 cm of elevation loss in the 50 years since embankment construction (Table 2).

2.3 Discussion

The relative sea-level calculation for the pristine Sundarbans highlights the known condition of 0 cm/yr relative sea level rise. Sediment accretion on the natural tidal delta plain occurs during periods of overbank flow at high tide and the frequently flooded Sundarbans receives a continuous sediment supply. This sediment supply roughly balances the rise in eustatic sea level, compaction and tectonic subsidence, which all lower the land elevation relative to mean high water. While localized variability in accretion, subsidence and compaction may result in localized variability in relative sea-level rise rates, the mean values used in this study demonstrate that overall the pristine system is capable of balancing constructive and destructive processes in the tidal delta plain.

The relative sea-level calculation for the polder accounts for almost 1 m of the 1-1.5 m elevation offset documented on Polder 32. Embankments designed to prevent overbank flow appear to starve the landscape of a

constant sediment supply and inhibit the only mechanism for landscape construction (van Proosdij et al., 2006). Meanwhile, compaction, subsidence and eustatic sea-level rise contribute to the rise in relative sea-level documented on Polder 32. Compaction, which is the most difficult variable to constrain, was differentiated by Syvitski et al. (2009) into natural and anthropogenic components. Natural compaction includes the loss in void space due dewatering, grain packing realignment and oxidation of organic matter, whereas anthropogenic compaction includes volume change from underground oil, gas, and water extraction, human-influenced soil drainage and accelerated oxidation. Natural compaction values have not yet been documented in the G-B tidal delta plain but spatial and temporal variability almost certainly exist due to variations in stratigraphy. The use in this study of compaction values on Polder 32 that are double the compaction rates in the Sundarbans certainly introduces some error; however, the estimated value used here may still be an underestimation due to groundwater extraction and other anthropogenic activities. In addition to loss in void space, the one-time compaction event resulting from wood biomass removal at the time of deforestation is likely a critical component to the historical elevation loss recorded on Polder 32. Because mangrove roots typically extend much deeper in the soil (1-2 m), the calculated value implemented in this study is representative of consolidated root depth. This elevation loss associated with deforestation would have occurred within a few years to decades, thus the wood extraction calculation is included as a single event rather than a process occurring throughout the 50 year lifespan of the polder. Despite uncertainties associated with the estimated mean values used in this RSL calculation, this study demonstrates that a significant part of the elevation offset observed on Polder 32 is the result of impeded sediment delivery.

The rapid sediment accretion documented in cores on Polder 32 highlights the ability of the system to disperse sediment onto the landscape in the absence of embankment protection. Post-cyclone mean annual sediment accretion rates on Polder 32 are 20 cm/yr, but reach as high as 40 cm/yr in some locations. These tidal splay deposits reflect the two-year period of daily tidal inundation that followed embankment breaches, and are consistently underlain by a darker grey, organic-rich, silty soil with root casts that corresponds to the agricultural surface that existed prior to the period of tidal inundation. Geoeye imagery shows that areas of Polder 32 that did not experience significant post-storm deposition were generally located at the distal reaches of the tidal splay features or where local embankments were repaired soon after the storm. Also, due to variations in the natural topography of the land, tidal splay deposit thicknesses were not removed from the land surface elevation data. Therefore, the elevation offset reported here, which represents a relative sea-level rise more than twice the IPCC's worst case scenario, is actually a very conservative estimate. Nonetheless, the mean sediment accretion rate documented after embankment failure is more than an order of magnitude faster than the background sedimentation rates in the Sundarbans and demonstrates the delta system's capacity to rapidly recover lost elevation (Allison and Kepple, 2001; Emery and Aubrey, 1989; Goodbred and Kuehl, 2000; PSMSL, 2013).

3. Tidal Delta Plain – Processes and Morphology

3.1 Approach and Methods

One of the greatest threats to people living in coastal regions is storms, such as Cyclone Aila which caused five major breaches of the embankments protecting the western margin of Polder 32. Bangladesh is affected by a tropical cyclone approximately once every two years, which makes understanding how and why embankment failures occur important for managing the future storm threat to poldered regions. Documenting the patterns of historical channel migration and bank erosion can potentially link points of shoreline instability to points of embankment failures on Polder 32 following cyclone Aila.

Changes in shoreline morphology on Polder 32 were observed via Ikonos, Worldview, and GeoEye images obtained prior to and following the landfall of Cyclone Aila in May 2009. Pre-cyclone shoreline morphologies were obtained from October 2001 Ikonos and April 2009 Worldview imagery of the polder. The post-cyclone shoreline morphology was obtained from GeoEye imagery of Polder 32 in 2011. The high water line, visible on the landscape in each of the three images, was used to digitize the shorelines in all images using ArcGIS. Digitization of shorelines revealed the progression of shoreline retreats, bank erosion and channel migration in the decade leading up to embankment breaches.

3.2 Results

Digitized Polder 32 shorelines from 2001 (yellow) and 2009 (orange), prior to Cyclone Aila, and 2011 (red), after Cyclone Aila, reveal that 50-200 m of bank erosion occurred along the west-northwest margins of the polder (Fig. 12). Shoreline digitizations also reveal additional channel meandering at two of the five breach locations, with notable point-bar development and cut-bank erosion in the decade prior to embankment breaches (Fig. 12). Four of the five breaches also occurred at the mouths of former tidal channels blocked by the embankments (Fig. 12).

3.3 Discussion

While the exact mechanism of embankment failure remains uncertain, these observations, coupled with the tidal splay deposits recovered in sediment cores and visible in Google Earth imagery from the polder, suggest that the embankments likely failed through undermining or collapse as a consequence of historical bank erosion coupled with surge-driven seepage and lift in the shallow sands. This same mechanism, as opposed to embankment overtopping, is similar to that cited for the London Avenue breaches that occurred in New Orleans during Hurricane Katrina and produced similar tidal scours and splay deposits (Nelson and Leclair, 2006; Ozkan et al., 2008). Within months of Cyclone Aila several of the breaches had been repaired, but poor build quality led to nearly complete failure of the embankments again in early 2010 (United Nations, 2010). Although the history of embankment repair has been complicated, 18 to 24 months passed before most of the breaches were soundly fixed, with the largest remaining unrepaired as of early 2013. The duration of flooding noted in imagery supports the evidence found in the sediment record of two years of tidal inundation.

4. Natural vs. Human-Modified Landscapes

4.1 Approach and Methods

Tidal channels dissect the delta platform and are the primary conveyers of sediment onto the landscape. While rates of sediment delivery and compaction differ between the human-modified and pristine environments, the two landscapes have in common the influence of semi-diurnal tides. This study has already demonstrated that sediment-laden tidal channels in this region are capable of conveying an average of 20 cm/yr of sediment onto the landscape when accommodation space is available; therefore, evolution of the tidal delta plain is a function of tidal water levels. Documenting the water levels relative to the landscape elevations of the human-modified and pristine environments is crucial for understanding the differences in evolution of these two landscapes.

In this study, a Schlumberger CTD-Diver, capable of logging water level, conductivity, and temperature, was deployed in the tidal channel adjacent to the eastern margin of Polder 32 within the Sundarbans (Fig. 13). The CTD-Diver was suspended inside a PVC pipe with perforated walls, which allowed water to flow around the instrument while keeping in the instrument in an upright position within the tidal channel (Fig. 13). The level of the instrument in the water column was included in the GPS elevation survey so that water levels and landscape elevations are relative to the same datum. The instrument was deployed from March 2012 to February 2013 and collected water level, temperature and conductivity data through the dry season and high-discharge monsoon season.

4.2 Results

The hydrologic dataset obtained from the instrument (Fig. 14) is essential to establishing a link between tidal fluctuations and sediment delivery to the delta platform by documenting the position of the platform relative to high tide levels. In the roughly 2-year period prior to embankment repair, the polder's low elevation relative to the tidal frame ensured that it was flooded on every tide, twice daily, to a mean depth of 100 cm and a period of ~10 hours per tide (Fig. 15). By contrast, the nearby Sundarbans is inundated only on spring high tides and to a depth of ~20 cm for ~2 hours (Allison and Kepple, 2001) (Fig. 15). It is here that the profound impacts of long-term subsidence and sediment starvation on Polder 32 become acutely apparent. In this case the historical loss of elevation has severely exacerbated the effects of tidal inundation by increasing the tidal prism (volume of water moving on and off the landscape), accounting for the exchange of $\sim 62 \times 10^6$ m^3 of water through the breaches during each tidal cycle. By contrast the tidal prism would have been 4-fold smaller if Polder 32 were at the equilibrium elevation of the adjacent Sundarbans.

4.3 Discussion

The results of this four part study demonstrate that the elevation offset on Polder 32 is consistent and widespread. Relative to the Sundarbans and river bank terraces outside of the embankments, the polder has lost approximately 1.15 m of elevation in 50 years. Results of this study also indicate that the rate of relative sea level rise on the polder is 2 cm/yr, while the background rate of relative sea level rise is 0.5 cm/yr. This elevation offset is largely the product of sediment starvation as a result of embankment construction in the 1960s. However, embankment breaches following Cyclone Aila re-established the connection between the polder and tidal channels, and sediment delivery was restored to the once protected landscape. River-bank terrace elevations, which are at roughly the same elevation as the Sundarbans, support the finding that elevation loss is a consequence of embankment construction and sediment starvation. These narrow margins along the polder remain connected to the tidal channels and have aggraded at a pace comparable to that of local RSL rise and the adjacent natural landscape.

Together, long-term stability of the Sundarbans and the equilibrium elevation of river-bank terraces along the polder reflect the robust capacity for the G-B delta to disperse and aggrade sediment in response to even reasonably high rates of RSL rise. This capacity is further demonstrated by the rapid sedimentation that occurred after tidal inundation was temporarily reestablished on Polder 32 following Cyclone Aila. Such re-equilibration of sediment-starved landscapes can also be achieved through the local practice of *tidal river management*, which, for example, accounted for ~2 m of sediment accumulation following a controlled breach of the perennially flooded Dakatia Beel (Rahman, 1994)

The results of this study have been used to develop a conceptual model, which outlines the evolution of the pristine and human-modified environments. The first stage of the model demonstrates that in the Sundarbans, tidal fluctuations and sea level rise in the tidal channel are capable of maintaining a dynamic equilibrium with the subsiding and compacting landscape via sediment dispersal and accretion. However, human modification of the landscape by embankment construction has locally inhibited sediment delivery to the landscape, decoupling these interacting systems. In this case, the sediment-starved landscape has continued to subside and compact, but in the absence of sediment accretion, the elevation of the interior landscape has become offset relative to the river bank terraces that continue to be tidally inundated. With the land surface situated below mean high water, failures at previously weakened points in the embankment caused by a cyclonic storm surge to re-establish sediment delivery to the landscape and over time may allow the dynamic equilibrium between the land surface and tidal inundation to be restored.

Conclusions and Implications

Sediment flux and dispersal from tidal channels onto the landscape is one of the principal processes that determines the delta system response to environmental changes. The exceedingly high rates of sedimentation following the embankment breaches exemplify the efficiency with which the tides and G-B fluvial system can disperse sediment to areas of accommodation, particularly where space has been generated through anthropogenically enhanced RSL rise. In this case it was the ~1-m loss in relative elevation that set the potential for rapid accretion following Cyclone Aila. Furthermore, such low land-surface elevations are found not only on Polder 32 but most embanked islands in southwest Bangladesh, giving considerable concern for more widespread impact of breaches and flooding.

Beyond Polder 32, most other embanked areas of southwest Bangladesh have experienced a similar elevation loss and now lie well below mean high water. This circumstance highlights the vulnerability of human-modified regions of the G-B delta to increased sea levels as a result of inhibited sediment delivery. In total Bangladesh supports 123 polders that are maintained by over 5000 km of embankments**.** If inhibited sediment delivery has resulted in the widespread loss of elevation across the poldered regions, then the immediate threat to G-B tidal delta plain appears to be one of human-manipulation of the local environment rather than global climate change and sea-level rise. Moreover, if the rate of sea level rise continues to increase as predicted (IPCC, 2007) and subsidence rates remain within the estimates noted by Allison and Kepple (2001), then the elevation offset of the interior polder will become increasingly severe in the absence of a sediment supply to the landscape. This increased offset would result in a greater disequilibrium between the tidal channels and the landscape, which could increase the risk and severity of flooding and landscape waterlogging.

The silver lining for Bangladesh and the G-B delta remains the one billion tons of sediment delivered and, where so allowed, effectively dispersed onto the landscape. Ultimately the complex picture that emerges from these events contrasts the risk posed by rapid elevation loss in many embanked areas of the G-B delta with the natural system's resilience through rapid potential sediment aggradation, raising both concern and hope for the effective management of this densely populated region.

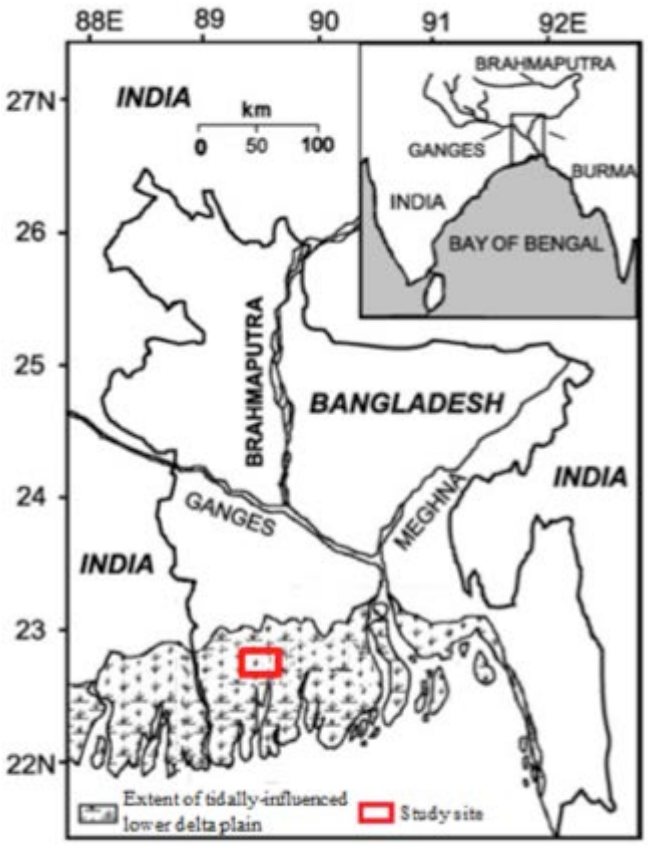

Figure 1. Map of the study area showing the locations of the Ganges and Brahmaputra Rivers and the tidally-influenced region of the G-B river delta. The study site is positioned within the red box (adapted from Allison *et al.*, 2003)

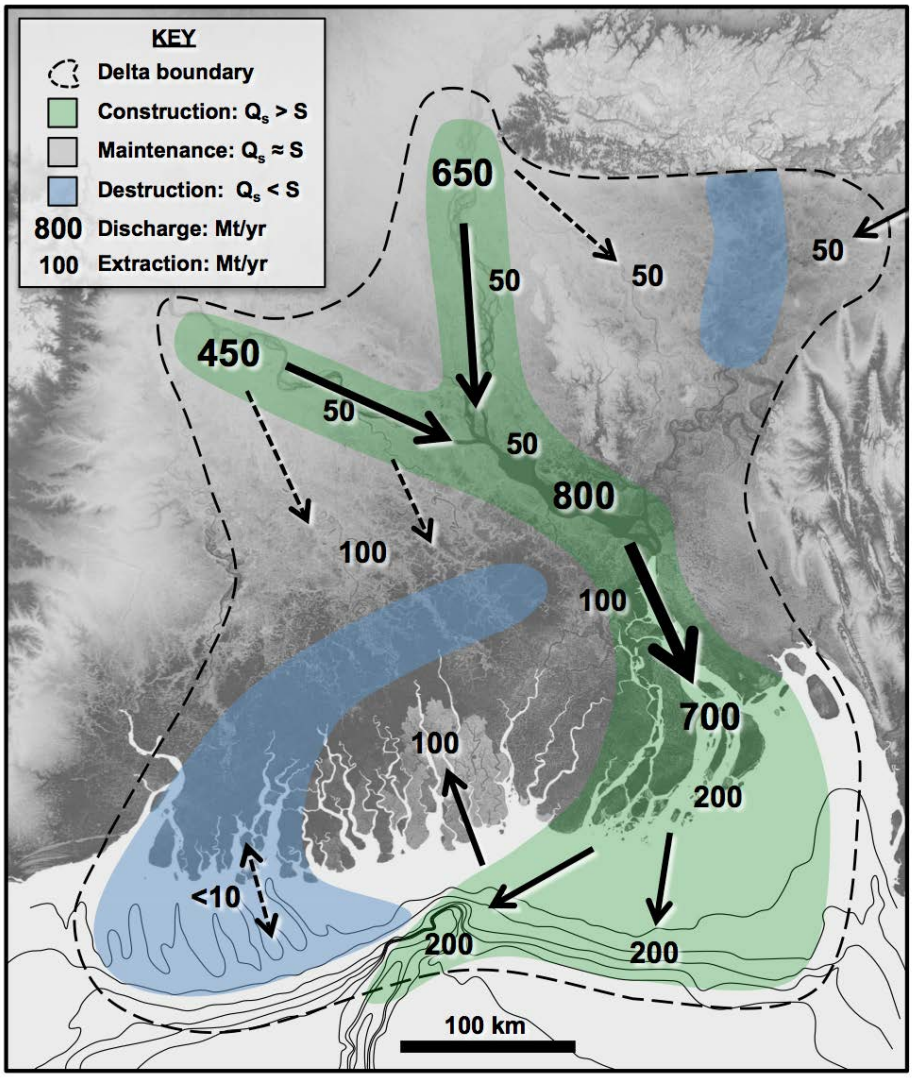

Figure 2. Map of the G-B delta showing the distribution of the ~1 billion tons of sediment transported annually from the Himalayas to the Bay of Bengal. Green regions on the map are in a constructive phase, with sediment accretion greater than subsidence rates. Blue regions on the map are in a destructive phase with rates of subsidence exceeding rates of sediment accretion. Gray regions of the map are in a maintenance phase with rates of sediment accretion approximately equal to rates of subsidence. The tidal delta plain is shown to be in a maintenance phase due to sediment delivery by tidal channels but the study area sits adjacent to a region of the delta in a destruction phase due to isolation from both fluvial distributaries and the tidal channel network (Wilson and Goodbred, in press).

Figure 3. Google Earth image of the G-B tidal delta plain, which is isolated from fluvial distributaries but is dissected by tidal channels extending from the Bay of Bengal to ~100 km inland. The darkest green portion of the landscape along the coast is the pristine Sundarbans mangrove forest. Islands immediately north of the Sundarbans are deforested and embanked to protect the landscapes from flooding. Areas north of the Sundarbans appear to be lower-lying and therefore waterlogged. The bright blue region just offshore of the G-B delta is suspended discharged from the river mouth and reworked by the tides (Google Earth, 2012).

Figure 4. Satellite imagery obtained in January 2009 (A) prior to Cyclone Aila. Note the expansive green spaces, which show a vegetated polder landscape. Satellite imagery from January 2011 (B) shows a tidally inundated and water-logged landscape caused by the embankment breaches during the May 2009 Cyclone Aila (Google Earth, 2009 and 2011).

Figure 5. Photograph of embankment on Polder 32 at high tide. Note that the interior landscape is situated 1-1.5 m below the high water line outboard of the embankment.

Figure 6. Photograph of the fixed GPS base station, with Trimble NetR9 receiver and Zephyr II antennas, which was cemented into the roof of a reinforced concrete school building (A). The base station was powered by a solar panel (B). Photograph of the rover used in the GPS elevation survey, also with a Trimble NetR9 receiver and a Zephyr II antenna, which was mounted on a fixed height tripod. (C).

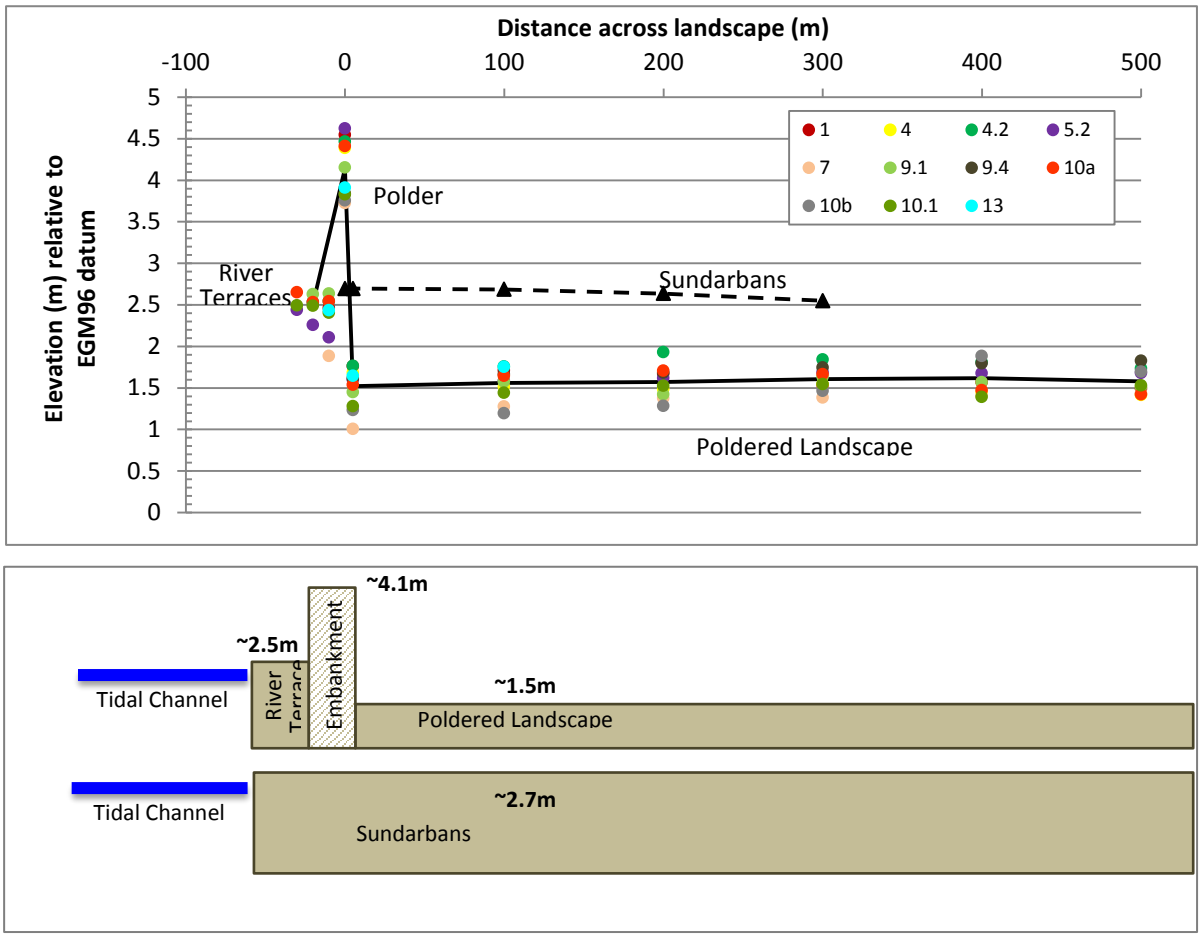

Figure 7. Results of the GPS elevation survey. Colored circles correspond to Polder 32 survey transects and black triangles correspond to the Sundarbans transect (A). The Sundarbans platform is positioned at +2.65 m relative to the EGM96 datum, and river terraces outboard of embankments on Polder 32 are positioned at approximately the same elevation, indicating that these frequently flooded regions are capable of maintaining equilibrium elevation with the tidal channels. Embankment heights across the polder range in elevation from +3.7 to +4.6 m. Cement embankment structures are generally positioned at higher elevations than earthen embankments, which explains the variability in embankment elevations. The poldered landscape is positioned an average +1.5 m above datum, with minimum and maximum values resulting from variations in the natural topography and land-use practices. The local practice of borrowing sediment closest to the embankments during repairs has

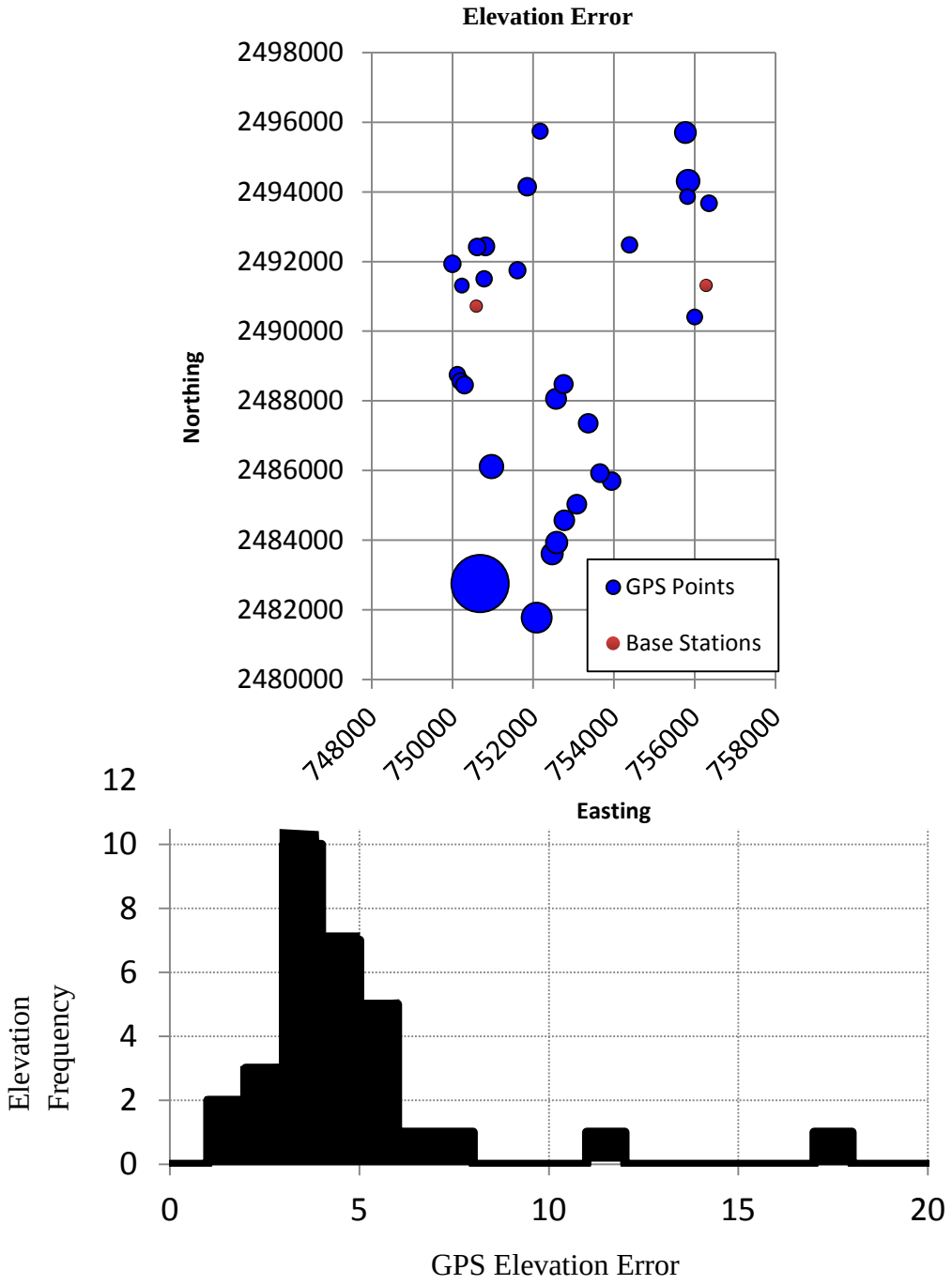

Figure 8. Map of position of GPS survey points with symbols proportional to the elevation errors (A). Base stations are indicated by red circles. Elevation errors ranged from 1-18 cmwith a mean elevation of 4cm.. The histogram of elevation errors for the GPS stations shows that only two points exceeded errors of 10cm (B).

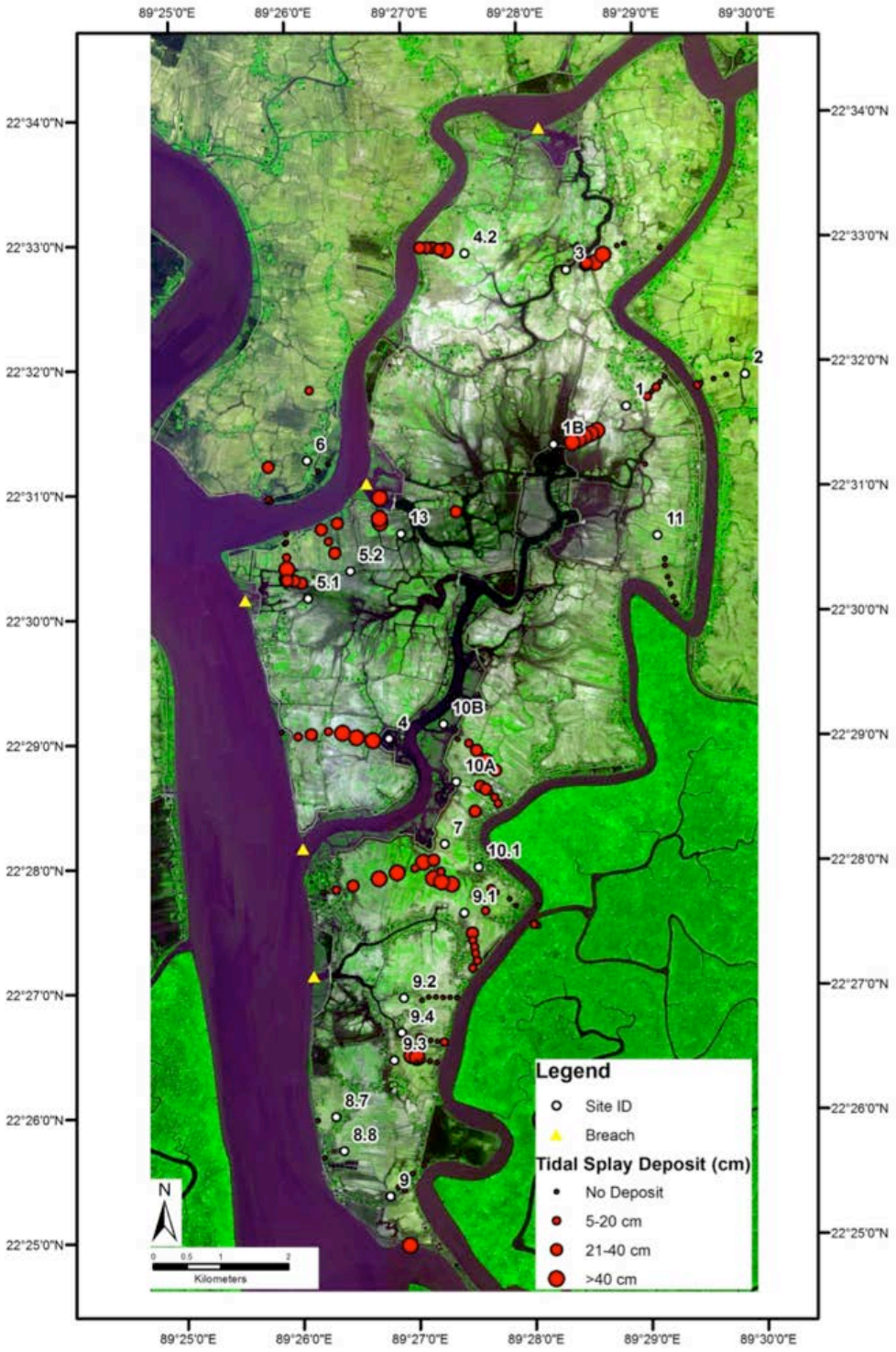

Figure 9. 2012 GeoEye image of Polder 32 showing GPS elevation survey and sediment core transects. The sizes of red circles are scaled to represent the thickness of tidal splay deposit found in each location. Regions of channel scour and broad tidal splay deposits indicated by black arrows, formed during the two years of tidal inundation following Cyclone Aila.

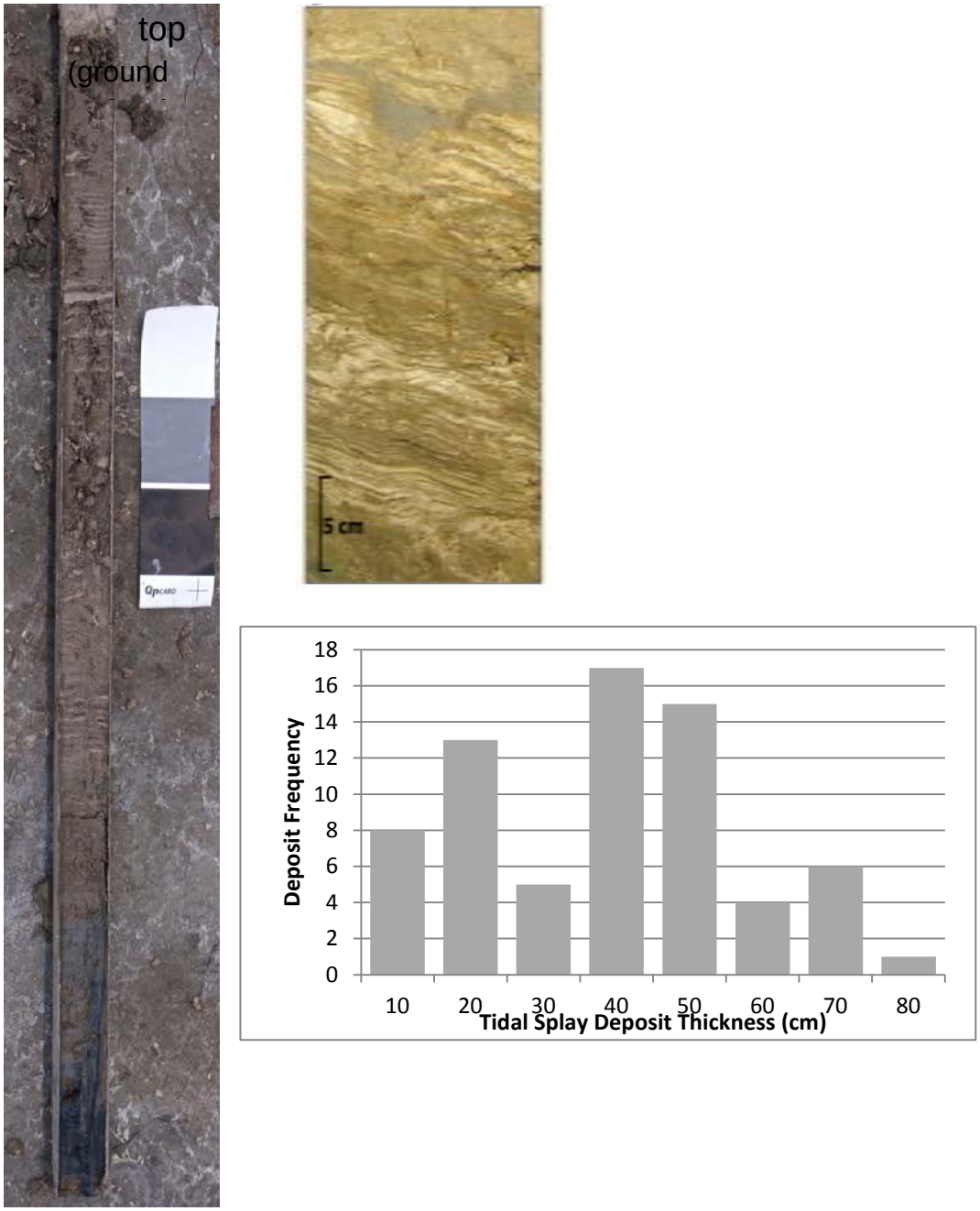

Figure 10. Photo of a sediment core showing silt and fine sand tidal laminites deposited during post-cyclone tidal inundation. Deposits in this image are 40 cm thick and overlie a gray, reducing soil horizon comprising the upper 10 cm of the pre-cyclone agricultural surface (A). Photograph of a 70-cm tidal splay deposit (B). A histogram showing the distribution of tidal splay deposit thicknesses on Polder 32 (C).

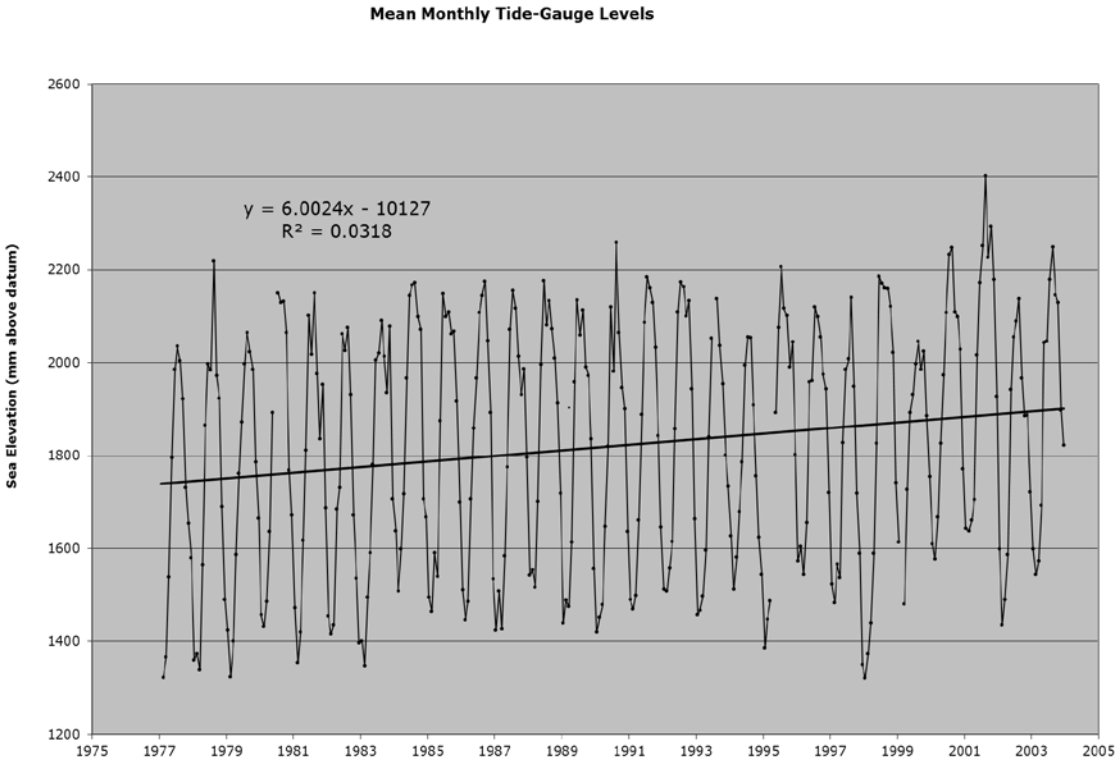

Figure 11. Bangladesh coastal tide gauge record from 1975 to 2005, which shows a relative sea level rise of 6 mm/yr. This rate accounts for rates of eustatic sea level rise, compaction and subsidence in the pristine environment.

Table 1. Root volume calculations from five species of mangroves in the Sundarbans.

Tree species	**dbh (cm)**	**dbh^2 (cm^2)**	**W_R (kg)**	**W_v (m^3)**
Sundri	51	2601	1267.9	1.2
Heritiera fomes[5]	79	6241	3349.8	3.2
ρ = 0.97 t/m3 to 1.1 t/m^3	78	6084	3256.4	3.1
	45.4	2061.16	979.4	0.9
	68	4624	2401.3	2.3
	54	2916	1439.5	1.4
	49	2401	1160.2	1.1
Cedar Mangrove (Passur)	122	14884	5384.3	9.0
Xylocarpus mekongensis[4]	156.2	24398.44	9319.3	15.5
ρ = ~0.6 t/m^3	92	8464	2877.5	4.8
	143	20449	7660.5	12.8
	66	4356	1376.6	2.3
	99	9801	3386.3	5.6
	49	2401	710.6	1.2
	110	12100	4278.6	7.1
	75	5625	1828.3	3.0
	129	16641	6094.2	10.2
	145	21025	7900.4	13.2
	163	26569	10244.0	17.1
	84	7056	2351.3	3.9
	115	13225	4722.4	7.9
	87	7569	2541.8	4.2
	93	8649	2947.4	4.9
	76	5776	1882.9	3.1
	81	6561	2168.9	3.6
	72	5184	1669.9	2.8
White/Grey Mangrove (Baen)	248.8	61901.44	26193.8	43.7
Avicennia sp.[4]	121	14641	5286.8	8.8
ρ = ~0.6 t/m^3	135	18225	6741.4	11.2
	92	8464	2877.5	4.8
	109	11881	4192.7	7.0
	102	10404	3618.3	6.0
	134	17956	6631.1	11.1
Large-leafed Orange Mangrove (Kankra)	103	10609	4241.7	6.1
Bruguiera gymnorrhiza[4]	80	6400	2420.5	3.5
ρ = ~0.7 t/m^3	62	3844	1374.5	2.0
Mangrove apple (Keora)	172	29584	11542.1	19.2
Sonneratia apetala[4]	147	21609	8144.3	13.6
ρ = ~0.6 t/m^3	110	12100	4278.6	7.1
	142	20164	7542.1	12.6

Table 2. Relative annual changes in local land-surface elevation and sea levels in the pristine Sundarbans and adjacent poldered landscape.

	Pristine			Poldered
	mean	min	max	mean
A (cm/yr) [12-14]	1.1	0.5	2.0	0
ΔE (cm/yr) [24]	0.3	0.2	0.4	0.3
C (cm/yr) [estimated]	0.4	0.2	0.8	0.8
M (cm/yr) [25,26]	0.4	0.1	0.8	0.4
ΔRSL (cm/yr)	0	0	0	-1.5
W	-	-	-	20
ΔRSL over 50 yr (cm)	0	0	0	-95

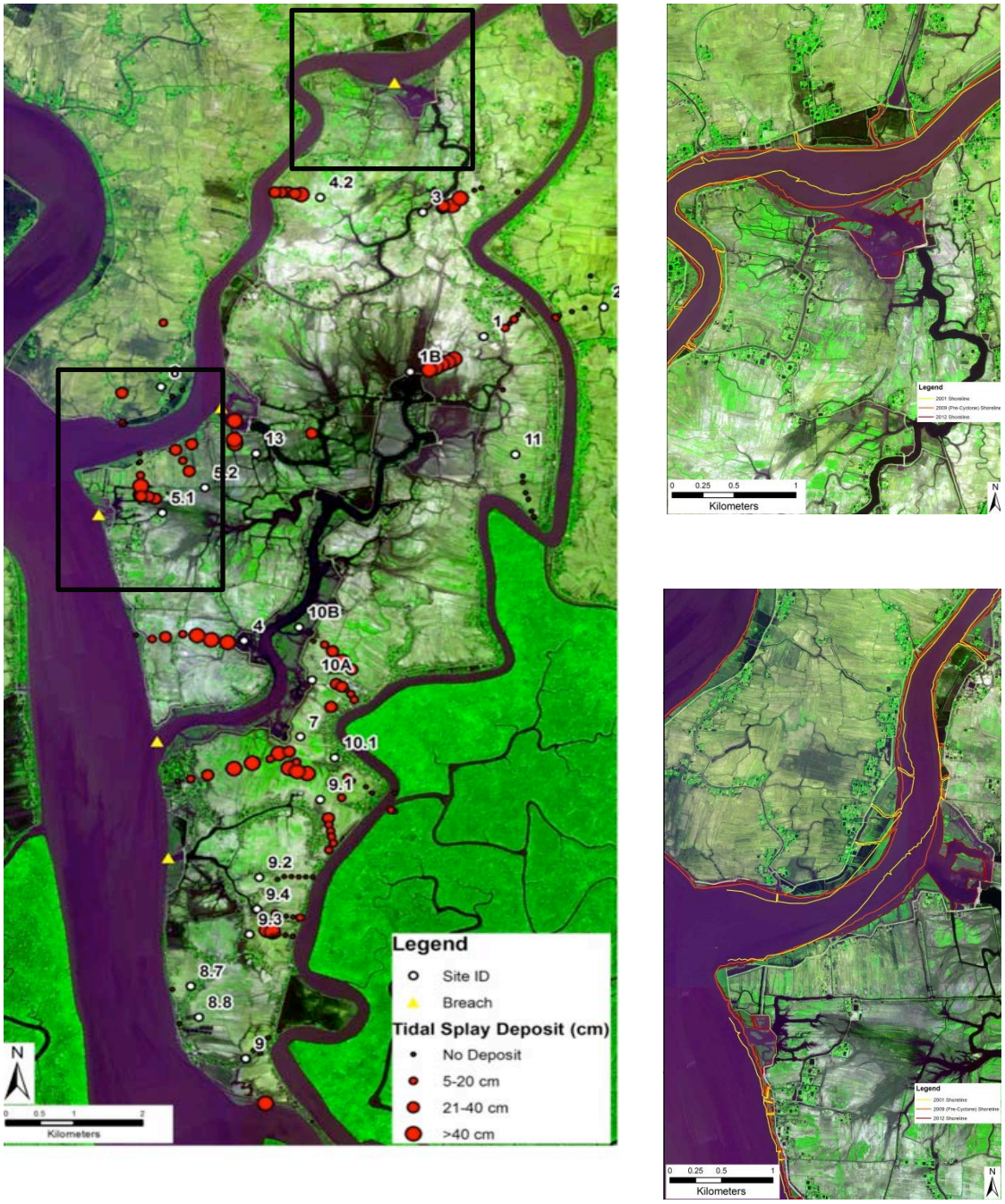

Figure 12. Breach locations and tidal splay deposits on Polder 32 (A). Expanded views of shoreline morphologies in 2001, 2009, and 2011 showing 50 – 200 m of river bank erosion and channel migration.

Figure 13. Schematic of Schlumberger CTD Diver, which was suspended in a perforated PVC pipe to allow flow through of water (A). The CTD Diver was deployed in on the to the east of Polder 32 (B) in a tidal creek with the Sundarbans (C).

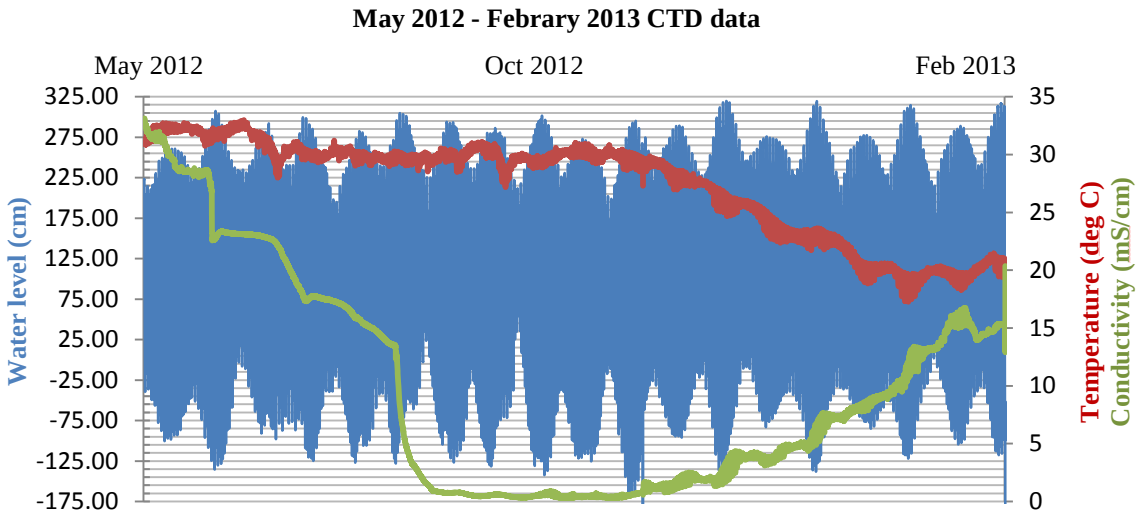

Figure 14. The hydrologic dataset obtained from the CTD Diver includes water level, temperature and conductivity data. Spring-neap tidal cycles are recorded, as well as changes in conductivity and temperature during the summer Monsoon season.

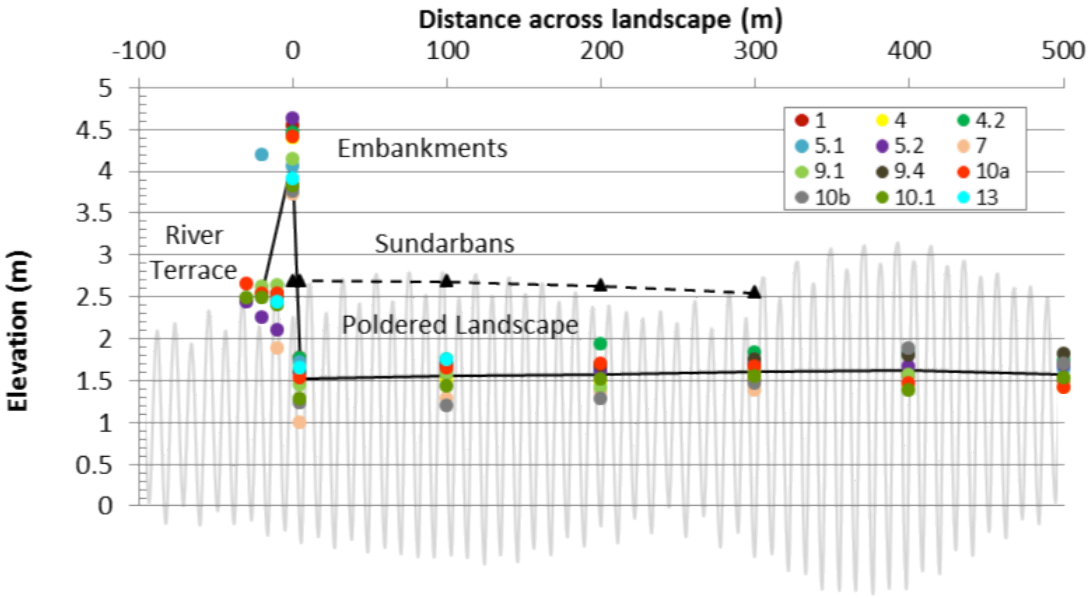

Figure 15. Superposition of a spring-neap tidal cycle onto the GPS elevation survey results shows that the Sundarbans and river bank terraces are flooded at 1/3 of all high tides for approximately two hours per day. In contrast, the poldered landscape is flooded at all high tides for approximately 10 hours per day in the absence of embankments. These results corroborate the average 20 cm/yr sedimentation rates documented on Polder 32 during the two year period of tidal inundation.

REFERENCES

Allison, M., Kepple, E., 2001. Modern sediment supply to the lower delta plain of the Ganges-Brahmaputra River in Bangladesh. Geo-Marine Letters 21, 66–74.

Allison, M.A., 1998. Historical changes in the Ganges-Brahmaputra Delta Front. Journal of Coastal ResearchJournal of Coastal Research 14, 1269–1275.

Allison, M.A., Khan, S.R., Jr, S.L.G., Kuehl, S.A., 2003. Stratigraphic evolution of the late Holocene Ganges – Brahmaputra lower delta plain 155, 317–342.

Bhuiyan, M.J.A.N., Dutta, D., 2012. Analysis of flood vulnerability and assessment of the impacts in coastal zones of Bangladesh due to potential sea-level rise. Natural Hazards 61, 729–743.

Bourne, J., 2000. Louisiana's Vanishing Wetlands : Going, Going... Science 289, 1860–1863.

Dasgupta, S., Huq, M., Khan, Z.H., Ahmed, M.M.Z. Mukherjee, N., Khan, M.F., Pandey, K., 2011. Climate Proofing Infrastructure in Bangladesh: The Incremental Cost of Limiting Future Flood Damage. Journal of Environment & Development 20, 167–190.

Day, J.W., Pont, D., Hensel, P.F., Ibañez, C., 1995. Impacts of sea-level rise on deltas in the Gulf of Mexico and the Mediterranean: The importance of pulsing events to sustainability. Estuaries 18, 636–647.

Emery, K.O., Aubrey, D.G., 1989. Tide Gauges of India. Journal of Coastal Research 5, 489–501.

Ericson, J.P., Vörösmarty, C.J., Dingman, S.L., Ward, L.G., Meybeck, M., 2006. Effective sea-level rise and deltas: Causes of change and human dimension implications. Global and Planetary Change 50, 63–82.

Giri, C., Pengra, B., Zhu, Z., Singh, A., Tieszen, L.L., 2007. Monitoring mangrove forest dynamics of the Sundarbans in Bangladesh and India using multi-temporal satellite data from 1973 to 2000. Estuarine, Coastal and Shelf Science 73, 91–100.

Goodbred, S.L., Kuehl, S.A., 1999. Holocene and modern sediment budgets for the Ganges-Brahmaputra river system : Evidence for highstand dispersal to flood-plain , shelf , and deep-sea depocenters. Geology 27, 559–562.

Herring, T.A., King, R.W., McClusky, S.C., 2010a. Documentation of the GAMIT GPS Analysis Software release.

Herring, T.A., King, R.W., McClusky, S.C., 2010b. GLOBK,Global Kalman filter VLBI and GPS analysis program.

IPCC, 2007. Climate Change 2007: Impacts, Adaptation, and Vulnerability : Contribution of Working Group II to the Fourth Assessment Report of the Intergovernmental Panel on Climate Change. Cambridge University Press, Cambridge, MA.

Jr, S.L.G., Kuehl, S.A., 2000. Enormous Ganges-Brahmaputra sediment discharge during strengthened early Holocene monsoon 1997–2000.

Komiyama, A., Poungparn, S., Kato, S., 2005. Common allometric equations for estimating the tree weight of mangroves. Journal of Tropical Ecology 21, 471–477.

Milliman, J.D., Syvitski, J.P.M., 1992. Geomorphic/Tectonic Control of Sediment Discharge to the Ocean: The Importance o f Small Mountainous Rivers1 100.

Nelson, S. a., Leclair, S.F., 2006. Katrina's unique splay deposits in a New Orleans neighborhood. GSA Today 16, 4.

Overeem, I., Syvitski, J.P.M., 2009. Dynamics and Vulnerability of Delta Systems.

Ozkan, S., Adrian, D.D., Asce, F., Sills, G.L., Asce, M., Singh, V.P., 2008. Transient Head Development due to Flood Induced Seepage under Levees. Journal of Geotechnical and Geoenvironmental Engineering 781–789.

PSMSL, 2013. Daily Tide Gauge Data: Hiron Point, Bangladesh [WWW Document]. http://www.psmsl.org.

Rahman, A., 1994. Beel Dakatia: The Environmental Consequences of a Development Disaster. University Press, Dhaka.

Rogers, K.G., Goodbred Jr., S.L., Mondal, D.R., 2013. Monsoon sedimentation on the "abandoned" tide-influenced Ganges-Brahmaputra Delta plain. Estuarine, Coastal and Shelf Science 131, 297–309.

Stanley, D.J., Warne, A.G., 1998. Nile delta in its destruction phase. Journal of Coastal Research 14, 794–825.

Syvitski, J.P.M., Kettner, A.J., Overeem, I., Hutton, E.W.H., Hannon, M.T., Brakenridge, G.R., Day, J., Vörösmarty, C., Saito, Y., Giosan, L., Nicholls, R.J., 2009. Sinking deltas due to human activities. Nature Geoscience 2, 681–686.

United Nations, 2010. Cyclone Aila: Joint UN Multi-Sector Assessment & Response Framework. New York.

Van Proosdij, D., Ollerhead, J., Davidson-Arnott, R.G.D., 2006. Seasonal and annual variations in the volumetric sediment balance of a macro-tidal salt marsh. Marine Geology 225, 103–127.